Highly tunable acoustic metamaterials based on a resonant tubular array

K. J. B. Lee,[1] Myoung Ki Jung,[2] and Sam H. Lee[2,*]
[1]*Department of Physics, Ewha Womans University, Seoul 120-750, Korea*
[2]*Institute of Physics and Applied Physics, Yonsei University, Seoul 120-749, Korea*
(Received 14 May 2012; revised manuscript received 3 November 2012; published 15 November 2012)

Recent theoretical studies demonstrated that waves can be steered in any desired fashion by using a suitable distribution of material parameters. However, the required parameters for acoustic transformations often surpass the ranges available from the metamaterials developed so far. We introduce a class of acoustic metamaterials based on standing waves in a tubular array and experimentally demonstrate continuous tuning of the compressibility in an unprecedentedly wide range from −8 to 6 relative to air at audio frequencies. Potential applications include the acoustic Luneburg lens and cloaking.

DOI: 10.1103/PhysRevB.86.184302 PACS number(s): 43.90.+v, 43.40.+s

I. INTRODUCTION

Metamaterials have extended ranges of available constitutive parameters for electromagnetic waves (permittivity ϵ and permeability μ) and for acoustic waves (density ρ and compressibility β) beyond the boundaries of conventional materials.[1–9] Single negative materials of four kinds[3,10–13] and double negative materials for both optics[4] and acoustics[14] have been realized. However, there still remain important yet unavailable areas in the Veselago's ϵ-μ space and its acoustic counterpart. The inaccessibility of these areas has impeded the fabrication of practical working devices of transformation optics and acoustics. The cloaking of a spherical space is an example. Despite extensive investigations and worldwide publicity, a truly working model of an invisibility cloak has not been reported yet: Strictly speaking, there were only two reports on experimental results regarding free waves, with one for microwave[8] and another for sound in water.[15] But both of them left out the impedance matching to the external space, allowing a strong reflection from the shell surface.

Constitutive parameters are changed from those of empty space by the action of unit-cell elements, which fill the space usually in the form of arrays. In many cases, two different kinds of unit-cell elements are used to control a pair of the constitutive parameters: To make double negative electromagnetic media, a split-ring resonator and long wires were used to form a composite structure.[4] In this case, the split-ring resonator was used to change permeability and the long wire was used for permittivity. A double negative acoustic metamaterial[16] was constructed by combining a Helmholtz resonator and a thin membrane, which were responsible for the control of the compressibility and the density, respectively. In many cases, each of the two elements controls its relevant parameter in a mutually orthogonal manner. For example, the shape and dimensions of the Helmholtz resonator affect the value of β only and the tension of the thin membrane changes ρ only.[16]

In transformation optics, the use of metamaterials lies in the capability of producing a continuous spectrum of positive parameters rather than negative ones. However, the whole range of positive parameters cannot be generated by these unit-cell elements. A split-ring resonator, in principle, is able to produce relative permeability from $-\infty$ to $1-F$ and from 1 to $+\infty$, but not in the range from $1-F$ to 1, where F is the geometrical factor.[3] The long wire and the thin membrane are not capable of creating the relative permittivity and the density larger than 1.[2,3] The Helmholtz resonator has a forbidden gap in the compressibility from 1 to $1+F$.[11]

Here we present an acoustic metamaterial which in principle generates the whole range of compressibility from $-\infty$ to $+\infty$ without any gap. Experimentally, we demonstrate tuning of compressibility in a range from −8 to 6 relative to air. The range is continuous without any gap in the middle and does not extend to ∞ only because of the dissipation.

II. STRUCTURE AND DYNAMICS

The proposed acoustic metamaterial, schematically shown in Fig. 1(a), consists of an array of branch tubes attached to a main duct. The spacing d between the tubes is much smaller than the wavelength. Each tube is equipped with a slidable plunger to adjust the length of the air column in the tube. In each tube, resonances occur at a series of frequencies as standing waves are formed. It turns out that in the lossless limit, the compressibility spans continuously from $-\infty$ to ∞ in each frequency interval between the resonances. Experimentally we obtained the range from −8 to 6 overming the shortage of the Helmholtz resonator system.

Previous investigations on acoustic systems[17,18] consisting of arrays of side-attached tubes similar to our structure did not include the effect of sequential formation of higher-mode standing waves in the side-attached tubes and overlooked the important feature we present in this paper. A very recent study by Garcia-Chocano *et al.*[18] on a structure consisting of a two-dimensional array of side tubes, for example, did not extend the focus of the investigation into the frequency range of the second standing-wave mode. Consequently, they reported an observation of the compressibility up to only 0.4, without any indication of overcoming the gap problem of the array of Helmholtz resonators.

Side-attached Helmholtz resonators change the effective compressibility because some portion of air in the duct sinks in or out of the neck of the Helmholtz resonator when pressure is applied. The effective compressibility starting with $1+F$ at

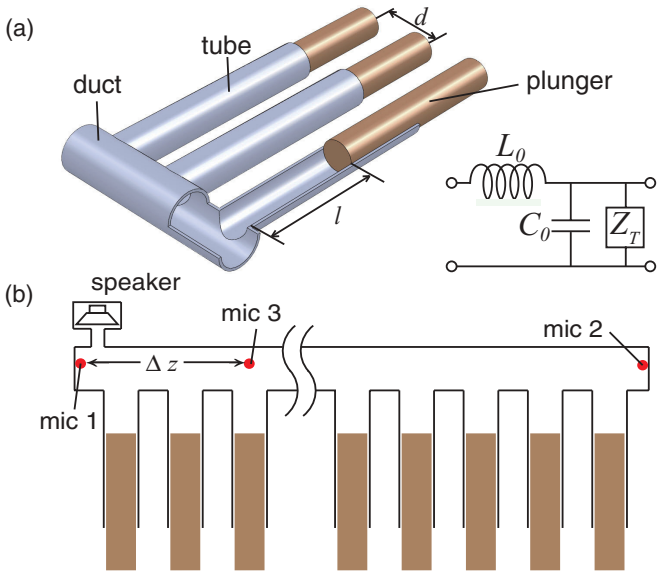

FIG. 1. (Color online) (a) Acoustic metamaterial exhibiting continuously tunable compressibility. (b) Experimental setup for determination of the dispersion relation.

zero frequency increases with frequency to reach the maximum at the resonance frequency. As the acoustic frequency passes through the resonance frequency, the phase of the motion of the air into the neck changes by 180° and the effective compressibility is abruptly dropped to a negative maximum value, which gradually rises up as the frequency is further increased to approach 1 asymptotically. As a consequence, the gap in compressibility from 1 to $1 + F$ is inevitably formed. Side-attached tubes have a similar effect on the effective compressibility of the duct, but a major qualitative difference comes from the fact that it has many resonance frequencies. Between two adjacent resonance frequencies, the effective compressibility changes continuously from $-\infty$ to ∞ in the lossless limit. As a result, the compressibility gap exhibited by the Helmholtz resonators disappears.

As sound propagates along the duct, the oscillating pressure causes the air to move in and out of the branch tubes. When air in a unit volume $V = S_D d$ of the duct experiences a net expansion ΔV_{net}, the pressure is changed by the amount $\Delta p = -B_0 \Delta V_{\text{net}}/V$, where S_D and B_0 are the cross section of the duct and the bulk modulus of air, respectively. Because of the motion of air into the tube, the net volume expansion ΔV_{net} is different from the apparent expansion ΔV by the volume displacement ΔV_{tube} of air into the tube, i.e., $\Delta V_{\text{net}} = \Delta V - \Delta V_{\text{tube}}$. Consequently, the effective compressibility defined as $\beta_r = B_0/B_{\text{eff}} = \Delta V/\Delta V_{\text{net}}$ can be expressed as

$$\beta_r = 1 + \frac{\Delta V_{\text{tube}}}{\Delta V_{\text{net}}}, \tag{1}$$

where B_{eff} is the effective bulk modulus.

To analyze the dynamics of air in the tube of length l with one end being closed, we consider Newton's equation and the wave equation for a displacement of air, $\xi(x,t)$, as follows:

$$\frac{\partial p_T}{\partial x} + \rho_T \frac{\partial^2 \xi}{\partial t^2} = 0, \tag{2}$$

$$\frac{\partial^2 \xi}{\partial x^2} - \frac{k_T^2}{\omega^2} \frac{\partial^2 \xi}{\partial t^2} = 0, \tag{3}$$

where p_T, ρ_T, and k_T are the pressure, the density, and the wave number in the tube, respectively. By imposing a boundary condition at the close end, $\xi(0,t) = 0$, it is straightforward to obtain

$$\frac{\xi(x,t)}{p_T(x,t)} = -\frac{k_T}{\rho_T \omega^2} \tan k_T x. \tag{4}$$

While the pressure at the open end of the tube is equal to that of the duct, i.e., $p_T(l,t) = -B_0 \Delta V_{\text{net}}/V$, the volume displacement of air in the tube, $\Delta V_{\text{tube}} = S_T \xi(l,t)$, becomes

$$\Delta V_{\text{tube}} = \Delta V_{\text{net}} \frac{S_T c_0}{\omega V} \tan \frac{\omega l}{c_0}, \tag{5}$$

where S_T is the cross-sectional area of the tube and $c_0 = \omega/k_T$ is the speed of sound in the air. Notably the volume displacement of air into the tube can be divergently larger than the net volume change ΔV_{net}. The effective compressibility in Eq. (1) is then rewritten as

$$\beta_r = 1 + \frac{S_T c_0}{\omega V} \tan \frac{\omega l}{c_0}. \tag{6}$$

This relation can also be derived independently using the well-established electrical transmission line analogy.[16,19,20] The equivalent electrical transmission line consists of an array of unit circuits, as shown in Fig. 1(a). The series inductor L_0 and the shunt capacitor C_0 represent the duct, whereas the shunt impedance Z_T represents the branch tube. The input impedance of a tube with a rigid termination is given by $Z_T = -iZ_0 \cot k_T l$, where Z_0 is the characteristic impedance of the tube.[21]

III. EXPERIMENTAL RESULTS

We derived Eq. (6) from the dynamics of a single cell. Clearly the characteristic periodicity in the frequency space stems not from the periodicity d of the tube array but from the resonant nature of each branch tube of length l. In other words, Eq. (6) still applies even when the tubular array is randomly spaced, as long as the average spacing remains d. When d is changed with fixed l, only the slope of each curve is changed. Stop bands with lower frequency edges occur periodically and the period is determined by l, independent of d: the spacing d affects only the width of each stop band. Similar results were reported by J. O. Vasseur *et al.*[22] for an electromagnetic comb structure.

Experimentally, we measured the dispersion relation, which can be expressed in terms of compressibility as

$$\omega = c_0 k/\sqrt{\beta_r}. \tag{7}$$

To measure the dispersion relation more precisely, instead of measuring wavelengths of traveling waves, we allowed total

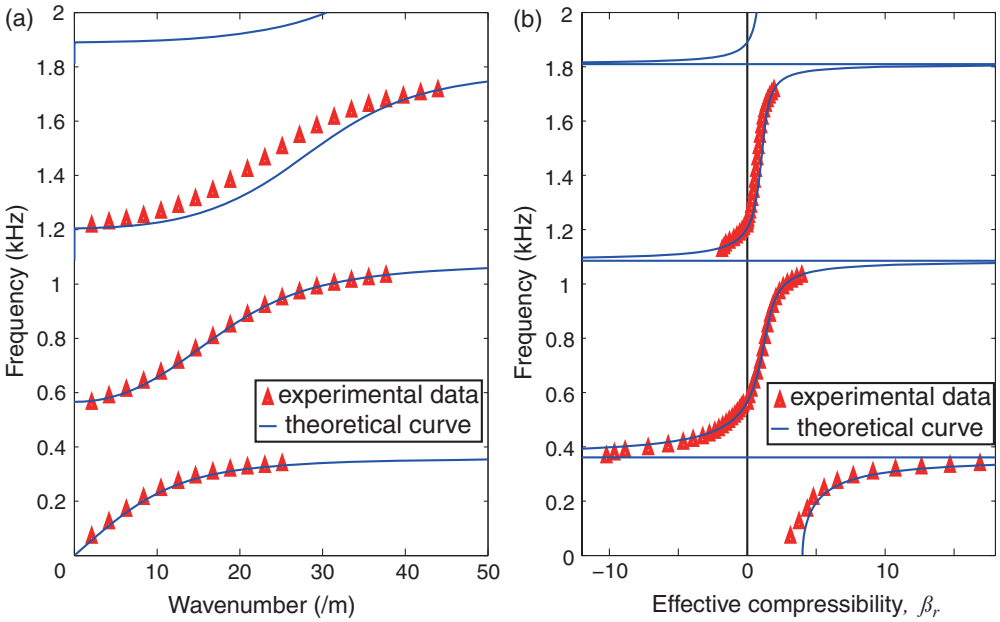

FIG. 2. (Color online) (a) Experimental dispersion-relation data and theoretical curves from Eq. (7). (b) Experimental data of effective compressibility agree well with the theoretical curve from Eq. (6).

reflections of the waves at the ends of the duct so that standing waves were formed in the duct at a series of frequencies. Note that these standing waves are the result of the superposition of oppositely propagating waves along the metamaterial and have nothing to do with the standing waves in the branch tubes. The dispersion relation was determined using the setup shown in Fig. 1(b). Both ends of the duct were closed and acoustic energy was supplied by the loudspeaker located at one of the ends. The amplitude and phase of the pressure were detected by three miniature microphones as in Fig. 1(b). Using the microphone 2, by detecting signal intensity as frequency was swept, the formation of standing waves in the duct was clearly observed in a series of resonance frequencies. The wave numbers k of the resonant waves are multiples of π/L, where L is the full length of the duct. By assigning these series of wave numbers to the measured resonance frequencies, we obtained the dispersion-relation data shown in Fig. 2(a). Theory and experiment agree well. For each branch, we were able to obtain the data only up to certain values of wave numbers due to dissipation.

Noticeably lower frequency edges of the stop bands occur periodically: In each stop band, we observed that the sound did not propagate but became evanescent along the duct. The decay constant κ of the evanescent wave was determined from the ratio of amplitude (A_1) at the microphone 1 to that (A_3) at microphone 3. The decay constant was obtained from $\kappa = (1/\Delta z)\ln(A_1/A_3)$, where Δz is the distance between microphones 1 and 3. Δz was typically about 100 mm. Since wave numbers were imaginary, $k = i\kappa$, the corresponding compressibilities $\beta_r = c_0^2 k^2/\omega^2$ were negative.

Experimental compressibility data, both positive and negative, are plotted together with the theoretical curve from Eq. (6) as a function of frequency in Fig. 2(b) using the parameters $S_T = 314\,\text{mm}^2$, $v_T = 340\,\text{m/s}$, $V = 24\,500\,\text{mm}^3$, $l = 235$ mm, and $L = 1500$ mm. These values correspond to the experimental setup. The experimental data agree excellently with the theoretical curve. Due to the different experimental errors for pass band and stop band, the apparent experimental data do not meet smoothly at zero compressibility. The widest compressibility span obtainable from the system was limited by the dissipation and this limitation becomes worse at higher-order resonances, as can be seen in Fig. 2(b). Clearly, it is best to choose the frequency interval between the first and second resonances.

For a fixed frequency, the compressibility can be tuned by sliding the plungers. The $\tan(\omega l/c_0)$ term in Eq. (6) diverges at the lengths satisfying $\omega l/c_0 = \pi/2, 3\pi/2, 5\pi/2, \ldots$, or whenever the length l becomes odd-integer multiples of $\lambda_T/4$. Figure 3(a) shows experimental data and the theoretical curve of Eq. (6) for the compressibility at an arbitrary fixed frequency of 550 Hz (corresponding to $\lambda_T = 618$ mm) as a function of l. Our experimental data again agree very well with the theoretical values. When $0 < l < 0.25\lambda_T$, β_r of our new metamaterial covers from 1 to 7.5. This range is enough to support devices such as the Luneburg and the Maxwell's fish-eye lenses.[23,24] On the other hand, when $0.25\lambda_T < l < 0.75\lambda_T$, we observed the compressibility spanning over the unprecedentedly wide range from -8.4 to 6.1 without any gap.

To demonstrate the potential applications of our new metamaterial, we constructed a profile of the tube lengths using the slidable plungers so as to create a linear distribution of compressibility along the duct, $\beta_r(z)$, theoretically from -6 to 6. The experimental data also follow the theoretical curve starting from $\beta_r = -6$ at one end, passing through zero in the middle, and continuously increasing to 6 at the

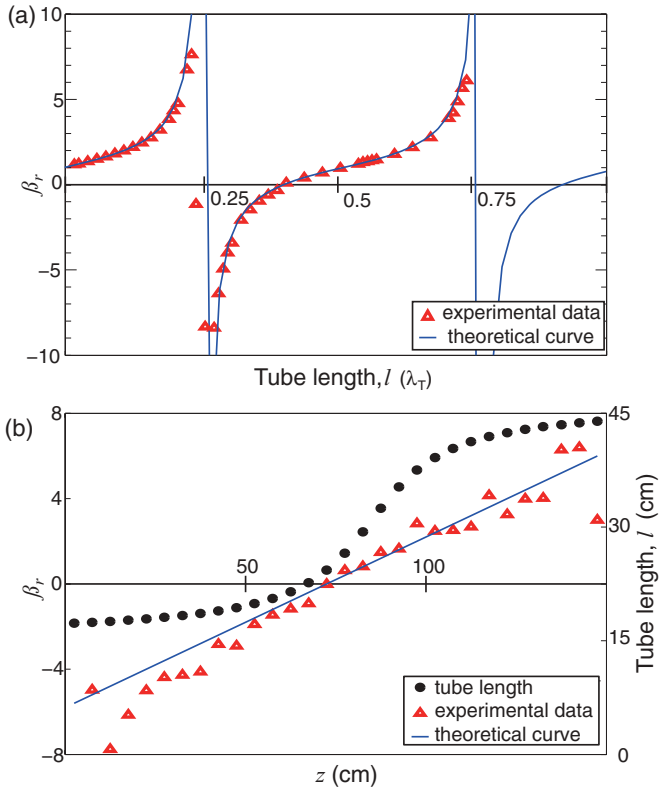

FIG. 3. (Color online) (a) Theoretical curves and the experimental data for the effective compressibility of the duct as a function of the tube length l. The theoretical curves diverge at odd multiples of quarter wavelength ($\lambda_T/4$) because of the term $\tan \omega l/c_0$ in Eq. (6). (b) A linear compressibility distribution was realized by constructing the tube length profile $l(z)$, as marked with the solid circles.

other end, as shown in Fig. 3(b). These data were obtained by measuring a phase change $\Delta\phi$ to the position change of detectors Δz to evaluate the wave number $k = \Delta\phi/\Delta z$. The direct measurement of the phase resulted in a much bigger error than the data in Fig. 3(a) and interference arising from partial reflection from both ends generated some wiggles. Nevertheless, the data follow the intended linear distribution reasonably well. It is noted that this linear distribution of the compressibility ranging from negative to positive values is extremely difficult to achieve in any other metamaterials developed so far.

As mentioned above, we experimentally confirmed that the effective density of the air in our metamaterial is not affected by the presence of the branch tubes, measuring the complex reflection coefficient R at the normal-tube/metamaterial boundary. The characteristic impedance Z of the metamaterial was obtained from the relation

$$\frac{Z}{Z_0} = \frac{1+R}{1-R}. \tag{8}$$

Table I lists the resulting experimental values of Z/Z_0 for the side tube lengths l of 185, 309, and 433 mm, respectively, at 550 Hz. The wave numbers k are also listed. The effective density ρ_{eff} is obtained by $\rho_{\text{eff}}/\rho_0 = (Z/Z_0)(k/\omega)c_0$. While

TABLE I. Experimental data for the characteristic impedances, wave numbers, densities, and compressibilities.

toprule l(mm)	185	309	433
Z/Z_0	$0.121 + 0.480i$	0.986	$0.471 + 0.047i$
$k(/m)$	$18.73i$	10.37	21.84
ρ_{eff}/ρ_0	$0.91 \pm 10\%$	$1.01 \pm 5\%$	$1.02 \pm 5\%$
β_r	−3.40	1.04	4.62

the compressibilities −3.4, 1.0, and 4.6, respectively, at these lengths are significantly different from each other, the effective densities remain equal to that of the normal air within the experimental error. The relatively larger experimental error for the $l = 185$ mm case, where the compressibility is negative, is due to the imprecision in the experimental determination of decay constant κ.

IV. CONCLUSIONS

It is important to note that the present structure is the first metamaterial without an inaccessible parameter gap occurring near 1 because the compressibility gap from 1 to $1 + F$ in the Helmholtz resonator system is not unique: The electromagnetic metamaterial consisting of split-ring resonators[3] has a permeability gap in the range from $1 - F$ to 1. The array of long wires[2] cannot make permittivity larger than 1. The array of I-shaped conductors[25] has the permittivity gap in the range from 1 to $1 + F$. Even the acoustic metamaterial consisting of an array of membranes[13] is not able to generate density in the range from 1 to ∞. Our work will provide a prototype for solving all of these gap problems.

Here, we performed experiments in air at audible frequencies, but as the dimensions are scaled down, our structure can be used for ultrasonic applications. Also, as water can be used instead of air, the wide-range tunability can be extended to underwater acoustics.

Most of the phenomena and devices for acoustic waves have their counterparts for electromagnetic waves. The Luneburg lenses for electromagnetic waves, for example, also need the same index distribution pattern from 1.41 to 1.[23,24] The ideas for many of the acoustic metamaterials, in fact, came from the electromagnetic counterparts developed previously. We expect that a reverse flow of ideas from acoustic metamaterials to electromagnetic metamaterials may also happen. Our work has the potential to be extended to electromagnetic waves since the electromagnetic counterpart for acoustic tubes exists: the wave guides.

ACKNOWLEDGMENTS

This work was partially supported by the National Research Foundation (Grant No. 2008-0062237) and Basic Science Research Program (Grant No. 2012-0002272) funded by the Ministry of Education, Science and Technology. The authors thank Oliver Wright for helpful discussions and comments on the paper.

*samlee@yonsei.ac.kr

[1] V. G. Veselago, Sov. Phys. Usp. **10**, 509 (1968).
[2] J. B. Pendry, A. J. Holden, W. J. Stewart, and I. Youngs, Phys. Rev. Lett. **76**, 4773 (1996).
[3] J. B. Pendry, A. J. Holden, D. J. Robbins, and W. J. Stewart, IEEE Trans. Microwave Theory Tech. **47**, 2075 (1999).
[4] D. R. Smith, W. J. Padilla, D. C. Vier, S. C. Nemat-Nasser, and S. Schultz, Phys. Rev. Lett. **84**, 4184 (2000).
[5] C. Caloz and T. Itoh, *Electromagnetic Metamaterials-Transmission Line Theory and Microwave Applications* (Wiley, New York, 2006), and references therein.
[6] J. B. Pendry, Phys. Rev. Lett. **85**, 3966 (2000).
[7] J. Zhu and G. V. Eleftheriades, Phys. Rev. Lett. **101**, 013902 (2008).
[8] D. Schurig, J. J. Mock, B. J. Justice, S. A. Cummer, J. B. Pendry, A. F. Starr, and D. R. Smith, Science **314**, 977 (2006).
[9] H. Chen, B.-I. Wu, B. Zhang, and J. A. Kong, Phys. Rev. Lett. **99**, 063903 (2007).
[10] D. Schurig, J. J. Mock, and D. R. Smith, Appl. Phys. Lett. **88**, 041109 (2006).
[11] N. Fang, D. Xi, J. Xu, M. Ambati, W. Srituravanich, C. Sun, and X. Zhang, Nature Mater. **5**, 452 (2006).
[12] S. H. Lee, C. M. Park, Y. M. Seo, Z. G. Wang, and C. K. Kim, J. Phys.: Condens. Matter. **21**, 175704 (2009)
[13] S. H. Lee, C. M. Park, Y. M. Seo, Z. G. Wang, and C. K. Kim, Phys. Lett. A **373**, 4464 (2010).
[14] S. H. Lee, C. M. Park, Y. M. Seo, Z. G. Wang, and C. K. Kim, Phys. Rev. Lett. **104**, 054301 (2010).
[15] S. Zhang, C. Xia, and N. Fang, Phys. Rev. Lett. **106**, 024301 (2011).
[16] Y. M. Seo, J. J. Park, S. H. Lee, C. M. Park, C. K. Kim, and S. H. Lee, J. Appl. Phys. **111**, 023504 (2012).
[17] M. S. Kushwaha, A. Akjouj, B. Djafari-Rouhani, L. Dobrzynski, and J. O. Vasseur, Solid State Commun. **106**, 659 (1998).
[18] V. M. Garcia-Chocano, R. Gracia-Salgado, D. Torrent, F. Cervera, and J. Sanchez-Dehesa, Phys. Rev. B **85**, 184102 (2012).
[19] F. Bongard, H. Lissek, and J. R. Mosig, Phys. Rev. B **82**, 094306 (2010).
[20] C. M. Park, J. J. Park, S. H. Lee, Y. M. Seo, C. K. Kim, and S. H. Lee, Phys. Rev. Lett. **107**, 194301 (2011).
[21] D. T. Blackstock, *Fundamentals of Physical Acoustics* (Wiley, New York, 2000).
[22] J. O. Vasseur, P. A. Deymier, L. Dobrzynski, B. Djafari-Rouhani, and A. Akjouj, Phys. Rev. B **55**, 10434 (1997).
[23] R. K. Luneburg, *Mathematical Theory of Optics* (University of California Press, Berkeley, CA, 1964).
[24] J. C. Maxwell, Cambridge and Dubling Math. J. **8**, 188 (1854).
[25] J. Shin, J.-T. Shen, and S. Fan, Phys. Rev. Lett. **102**, 093903 (2009).